Hartl, H., Elgamal A., *“Nicht lineare kontinuumsmechanische Modellierung vorgespannter Konstruktionen (Non Linear Modeling of Prestressed Structures based on a Continuum Mechanics Approach)”* (in English), Heft 45 / September 2000, Österreichische Vereinigung für Beton- und Bautechnik, Vienna, pp. 87-96

Helmut Hartl, Dipl.-Ing., TU-Graz, University of California San Diego
Ahmed Elgamal, Ph.D., Prof., University of California San Diego

Nicht lineare kontinuumsmechanische Modellierung vorgespannter Konstruktionen
Non Linear Modeling of Prestressed Structures based on a Continuum Mechanics Approach)

ABSTRACT: A finite element formulation based on 3D solid elements is developed for concrete with embedded 1D elements in order to represent the reinforcement and tendons. The concrete is modeled as a plastic material. Steel reinforcement/tendons are allowed to intersect the mesh in any arbitrary direction. The contribution of the rebars/tendons to the stiffness matrix is superimposed on the respective parent elements. Rebar stiffness contribution is integrated along its path within the parent element. No additional degrees of freedom are introduced for the reinforcement. Thus, the mesh design can be achieved without considering the reinforcement layout. Prestress is considered within an iterative procedure by utilizing the load balancing concept. Bond slip or tendon sliding can be modeled by introducing supplementary interface elements, after the displacement field has been computed. All loading sequences caused by the action of prestress can be simulated.

1 Introduction

If the FE-method is applied for a comprehensive assessment of a reinforced/prestressed concrete structure, the program must be able to account for the nonlinearity of the concrete and for the presence of the rebars. Thus, every single rebar has to be defined in the input phase. This might have been cumbersome in the past, but since CAD detailing is standard nowadays, this information is in general available in digital form. This digital form allows convenient accessibility to the finite element program. The merit of such a scheme is, that a design can be assessed computationally with no idealization necessary. This approach follows a clear trend in software engineering as well. The central database holds all the information related to the object of interest and each application retrieves the information from this database. Computing performance is not a primary limitation any more and case studies presented in this paper are very promising in this regard. A procedure for such a comprehensive nonlinear analysis based on a continuums mechanics approach is presented in this paper. The work is implemented into an existing *B*oundary *E*lement / *F*inite *E*lement program (*BEFE* [1]), which provides a useful pre and post-processing environment. Some tools for manipulating the reinforcement were added and an interface to a CAD program is in preparation [2].

When reinforced concrete structures are modeled based on continuum mechanics, there are three methods available for modeling the reinforcement: the smeared, the discrete, and the embedded approaches, Hofstetter [3]. The smeared approach is more suitable for homogenous distributed reinforcement, such as in wall panels. The quantities of the reinforcement are smeared uniformly over the element. The discrete approach represents the rebars by truss elements, that are connected to the mesh at the concrete element nodes. Hence, the mesh design becomes dependent on the reinforcement layout. This restriction may lead to unnecessarily small elements, or results in inaccuracy due to undesirable element aspect ratios. Within the embedded approach proposed by Elwi [4], these restrictions do not apply. The reinforcement is superimposed on the parent element with no additional degrees of freedom. Thus, reinforcement is allowed to intersect the parent elements without restrictions, and the mesh design can be done independently of reinforcement layout. This method is employed in this program and described in section 2.

Prestress is widely accounted for by utilizing the load balancing concept, introduced by Lin [5] and Leonhard [6]. This concept can be applied to the developed finite element approach and all equilibrium equations can be derived accordingly as presented here in section 3.

Accounting for bond slip with interface elements in the conventional way proposed by Ngo [7] and Schäfer [8] is only possible within the discrete approach. However, it would increase the global stiffness matrix size dramatically. Literature is hardly found regarding general applicability utilizing this

method. Within the embedded approach, the same displacement field has to be assigned to the concrete and to the rebars (perfect bond is obtained), since no additional degrees of freedom are introduced for the reinforcement. Currently, no model for bond slip within the embedded approach appeared to be available (Hofstetter [3]). Recommendations were made to modify the constitutive equations empirically for concrete or steel in order to simulate bond slip. Hartl [9] proposed a model capable of accounting for anchorage loss, but unable to account for the slip. Here a procedure for incorporating bond slip within the embedded approach is shown. This procedure (shown in section 4) is also able to compute the tendon elongation during the prestressing action. The mechanical sequences during most common prestressing actions and numerical case studies are discussed finally.

2 Embedded Modeling of Rebars/Tendons

The reinforcement is incorporated by one-dimensional bars within the parent element at the exact location within the considered domain. This reinforcement can be curved and even the start/endpoint of a rebar is not restricted to the concrete element boundaries. Defining the reinforcement in global coordinates for each element is a time consuming job. Here, the information regarding the rebars can be provided independent of the mesh and a preprocessing routine detects the intersection of the reinforcement with the faces of the parent 2D or 3D elements. In the general case these are intersections of a parabola with a higher order surface, Hartl [9].

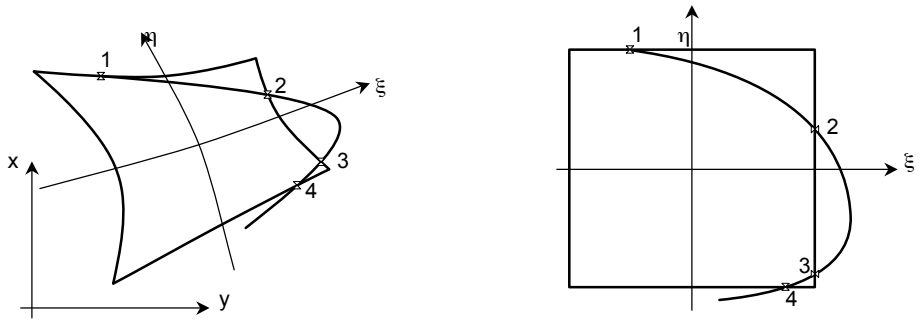

a) Global configuration b) Local configuration

Fig. 1 Intersection points of the reinforcement with the element faces

The integration of the stiffness matrix is done within the same theoretical framework for the concrete and for the rebars. The concrete stiffness is represented by the first term of Eq. (1), and can be computed in a straightforward fashion. The stiffness of the rebar is neither homogeneous nor isotropically distributed over the parent element, but available along the rebar only. Thus, integration for the rebar stiffness has to be performed along the rebar. Appropriate sample points for the numerical integration (Gauss points) have to be determined along the rebar. The orientation of the rebar at these points must be computed as well. The integration points of the rebars can be computed easily with respect to the global configuration. Then, a mapping procedure must be employed in order to obtain the integration points within the isoparametric configuration of the parent element. This is an inverse relation compared to the standard mapping scheme within the finite element method. It is not easily found, since the mapping matrixes are not square matrixes. Here, it is done by an optimization method, proposed by Elwi [4]. The robust multi-dimensional Newton root finding method, is employed. When the integration points within the local configuration of the parent element are known the element stiffness matrix can be computed

$$K^e = \int_{V,parent} \mathbf{B}_p^T \mathbf{D}_p \mathbf{B}_p dV_{parent} + \sum_{RB} A_r \int_{l_r} \mathbf{B}_p^T \mathbf{T}_{\varepsilon,gl}^T \mathbf{D}_r \mathbf{T}_{\varepsilon,gl} \mathbf{B}_p dl \qquad (1)$$

where
- $\mathbf{B}_p$ strain displacement matrix for the 2D/3D parent element
- $\mathbf{D}_p$ elasticity matrix for the parent element
- V considered volume
- A_r cross section area of the rebar
- RB number of rebars within the considered parent element
- $\mathbf{D}_r$ elasticity matrix for the reinforcement ($\mathbf{D}_{1,1}=E_s$, all other components = 0)
- $\mathbf{T}_{\varepsilon,gl}$ strain transformation matrix from the **g**lobal to the **l**ocal axis, (e.g. Boresi [10])

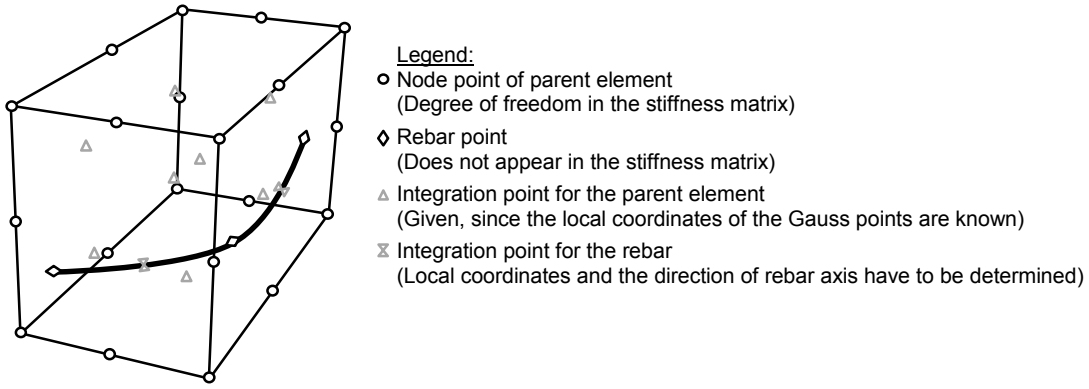

Fig. 2 Embedded reinforcement

3 Accounting for Prestress

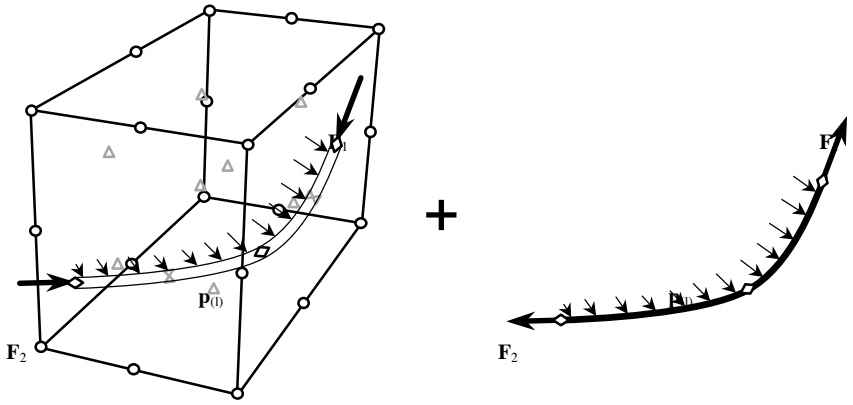

Fig. 3 Forces applied on the concrete and on tendon within the load balancing concept

Prestress is taken into account in any conventional analysis within the load balancing concept proposes by Lin [5] and Leonhardt [6]. Applying this load balancing concept to the element in Fig. 3 the equilibrium of virtual work for the concrete element can be written as (Hofstetter [3])

$$-\int_{V_p} \delta\mathbf{e}\cdot\mathbf{s}_p\, dV_p + \int_{V_p} \delta\mathbf{u}\cdot\mathbf{b}\, dV_p + \int_{S_p} \delta\mathbf{u}\cdot\mathbf{t}\, dV_p + \int_{l_{duct}} \delta\mathbf{u}_{(l)}\cdot\mathbf{p}_{(l)}\, dl + \delta\mathbf{u}_{(1)}\cdot\mathbf{F}_{(1)} + \delta\mathbf{u}_{(2)}\cdot\mathbf{F}_{(2)} = 0 \tag{2}$$

In Eq. (2) the first term refers to the internal stresses in the concrete, the second and the third term refer to body forces and to surface traction respectively on the concrete element. The forces exerted from the tendon to the concrete are accounted for by the terms in the second line of Eq. (2). The fourth term refers to the line load along the duct, and finally the last two terms account for the axial force applied on the concrete.

For the tendon in Fig. 3 the equilibrium equation of virtual work is

$$-A\int_{l_{duct}} \delta\varepsilon_s\cdot\sigma_s\, dl - \left[\int_{l_{duct}} \delta\mathbf{u}_{(l)}\cdot\mathbf{p}_{(l)}\, dl + \delta\mathbf{u}_{(1)}\cdot\mathbf{F}_{(1)} + \delta\mathbf{u}_{(2)}\cdot\mathbf{F}_{(2)}\right] = 0 \tag{3}$$

where the first term refers to the work done by the tendon, and the other three terms are the same as in Eq. (2). However on the tendon, these forces act in the opposite direction compared to the concrete element (Fig. 3). Hence, if the equilibrium for the combined element is considered, these latter three terms cancel out, since equilibrium is stated by the sum of Eq.(2) and (3).

The equilibrium is represented by

$$-\int_{V_p} \delta\mathbf{e}\cdot\mathbf{s}\; dV_p + \int_{V_p} \delta\mathbf{u}\cdot\mathbf{b}\, dV_p + \int_{S_p} \delta\mathbf{u}\cdot\mathbf{t}\, dV_p - A\int_{l_{duct}} \delta\varepsilon_l \cdot\sigma_s\, dl = 0 \qquad (4)$$

Therefore, prestress can be taken into account by consideration of the tendon stress only, where

$\delta\mathbf{e}^T$	$\left[\delta\varepsilon_{xx},\delta\varepsilon_{yy},\delta\varepsilon_{zz},\delta\varepsilon_{xy},\delta\varepsilon_{yz},\delta\varepsilon_{zx}\right]$	incremental strain
$\mathbf{s}_p^T$	$\left[\delta\sigma_{p,xx},\delta\sigma_{p,yy},\delta\sigma_{p,zz},\delta\sigma_{p,xy},\delta\sigma_{p,yz},\delta\sigma_{p,zx}\right]$	stress on parent element
$\mathbf{u}^T$	$\left[\delta u_x,\delta u_y,\delta u_z\right]$	incremental deformation
$\mathbf{b}^T$	$\left[\delta b_x,\delta b_y,\delta b_z\right]$	body forces on the parent element
$\mathbf{t}^T$	$\left[\delta t_x,\delta t_y,\delta t_z\right]$	traction forces on the parent element
$\mathbf{p}^T$	$\left[\delta p_l,\delta p_n,\delta p_b\right]$ (l,n,b…moving trihedral)	traction forces on the rebar
$\delta\varepsilon_l$	$\mathbf{T}\cdot\delta\mathbf{e}$	first component of strain increment along dl
σ_s		steel stress

The steel stress is obtained by relating the steel strain to the constitutive equation of the rebar. Within the embedded approach, steel strain is computed from the displacement field of the parent element. Thus, this computed steel strain must be modified by the strain, which is applied during the prestress action. This strain is either given direct as input data, or it will be computed from the applied prestressing force. The strain at a rebar point with respect to global axis is

$$\mathbf{e} = \mathbf{B}_p \cdot \mathbf{u} \qquad (5)$$

This strain is rotated to the local configuration of the rebar by

$$\mathbf{e}_{lc} = \mathbf{T}_{\varepsilon,gl} \cdot \mathbf{e} \qquad (6)$$

where the first component of $\mathbf{e}_{lc}$ is strain along the rebar (ε_l). The strain applied by the prestress action is added to ε_l. The obtained total strain is related to stress by the constitutive law for the steel. Secondly, ε_l has to be related to stress by the elasticity matrix, that is employed for the rebar in the stiffness matrix. The difference can be considered as residual stress and has to be reapplied on the domain as residual forces within an iterative scheme.

The prestress action can be accounted for without any simplification needed. However, slip situations during the prestress action or later when external load is applied, cannot be accounted for.

4 Supplementary Interface Model

The displacement field in the domain is controlled by the global stiffness matrix, which is restricted to perfect bond. On the material level, continuous interface elements are introduced along the rebar. Arising bond slip is mapped as residual force. The demand on computing time will obviously increase somewhat, but this model needs not be applied to every rebar. It can be assigned to certain rebars only. For other rebars within the same domain, the assumption of perfect bond or anchorage loss (Hartl [9]) might be sufficient.

The basic idea of this approach is briefly illustrated below on a truss analogy as shown in Fig. 4. The truss members are the rebars; and the supports are the concrete. Since we account for slip, the supports are linked to the rebars by bond springs. We know from the FE-analysis the displacement field of the parent concrete element. It can be considered as prescribed displacements of the supports. These support displacements are now transferred to the rebars by bond springs. The arising relative displacement of a rebar support node and the adjacent rebar node is referred to as bond slip. The differences of the forces in the rebar elements now, compared to forces in these elements with rigid bond, are forces due to bond slip. These forces are mapped back as residual nodal forces of the parent element. From (2), (3) and (4) follows that the interface forces need not to be considered within the residual forces, since these forces cancel out.

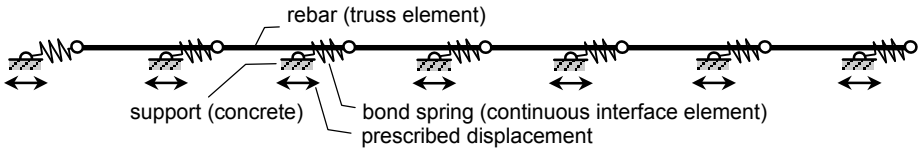

Fig. 4 Truss analogy of the supplementary interface model

This idea is now formulated in a form suitable for the Finite Element Method, according to the following steps

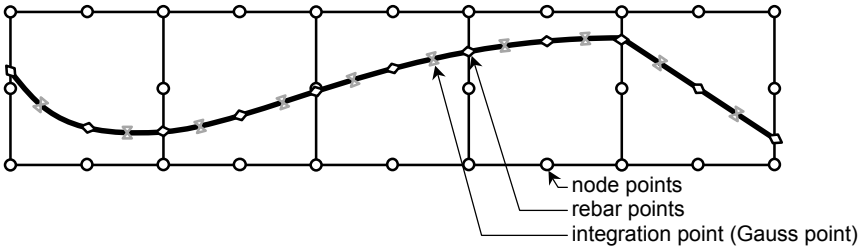

Fig. 5 Supplementary interface model

Let us apply the truss analogy to Fig. 5. A support by the parent concrete is assumed at each rebar point (<> in Fig. 5). This support is connected to the rebar by a bond spring (continuous interface) at the rebar point. The quantities are integrated at the Gauss points for the rebar. (>< in Fig. 5). Hence, the correction stresses due to bond slip will be computed at these integration points as well. The same shape functions employed for the rebars in global the domain are used for this bond slip computation. First, we have to compute the elongation along the reinforcement between two adjacent points. In FE-notation notation, Δl is the first component of the following vector

$$\Delta \mathbf{l} = \int_{\xi_n}^{\xi_{n+1}} \mathbf{T}_{\varepsilon,gl} \cdot \mathbf{B}_p \cdot \mathbf{u} \cdot J \cdot d\xi \tag{7}$$

where $d\xi$… isoparametric coordinates along the rebar J… Jacobian determinant for the rebar, and Δl is a scalar value containing the elongation between two adjacent rebar points.

In order to have the prescribed displacement for a specific rebar node available, we have to sum the elongations from the first node of this rebar up to the current rebar node.

$$u_n = \sum_1^n \Delta l \tag{8}$$

Next, the stiffness matrix of the rebar trusses must be computed

$$\mathbf{K}_{rebar} = A \int_{-1}^{+1} \mathbf{B}_r^T \cdot E \cdot \mathbf{B}_r \cdot J \cdot d\xi \tag{9}$$

where $\mathbf{B}_r$ strain displacement matrix for 1D rebar elements
E modulus number of the rebar

And the stiffness matrix of the bond element is

$$\mathbf{K}_{bond} = \int_{-1}^{+1} \mathbf{B}_b^T \cdot k \cdot \mathbf{B}_b \cdot J \cdot \phi \cdot \pi \cdot d\xi \tag{10}$$

where $\mathbf{B}_b$ strain displacement matrix for bond (interface) elements (analog to Beer [11])
k stiffness of the interface (=τ_b/u), see section 4.1)

All stiffness terms are available now. When mild steel is considered, the only loads applied are prescribed displacements. When the bars are prestressed, nodal loads apply in addition as discussed in section 5. However, the system can be solved now within an incremental iterative procedure and the displacements of the rebar node points will be obtained. The relative displacement between a rebar node and the according point in the parent element can be referred to bond slip.

To calculate from this bond slip the strain at the integration point is straightforward

$$\varepsilon_{slip} = \mathbf{B}_r \cdot \mathbf{u}_{rel} \tag{11}$$

where $\mathbf{u}_{\text{rel}}$ is relative displacement (slip)
The strain along the rebar at the identical point assuming rigid bond is obtained from the displacement field of the parent element

$$\mathbf{e}_{rigid\_bond} = \mathbf{T}_{\varepsilon,gl} \cdot \mathbf{B}_p \cdot \mathbf{u}_p \tag{12}$$

The strain in the rebar is now

$$\varepsilon_r = \varepsilon_{rigid\_bond} + \varepsilon_{slip} \tag{13}$$

The rebar strain has to be related to stresses by the constitutive law for the rebar. The difference in these stresses compared to those assuming rigid bond must be mapped as residual nodal forces.

4.1 Bond Slip Relation

In order to account for the different slip conditions which can occur, three different models for the bond slip condition are provided.

a) Interface of rebar with concrete or tendon with grout

For a bond condition which arises between steel and concrete or tendon and grout some models are available (Eligehausen [12], Modelcode 90 [13], Pochanart [14], Priestly [15]). The model implemented is primarily that proposed in Modelcode 90 since it is supposed to show a close agreement with the design code EC2. However some modifications are necessary in order to account for stresses acting perpendicular to the bar and for unloading/reloading conditions.

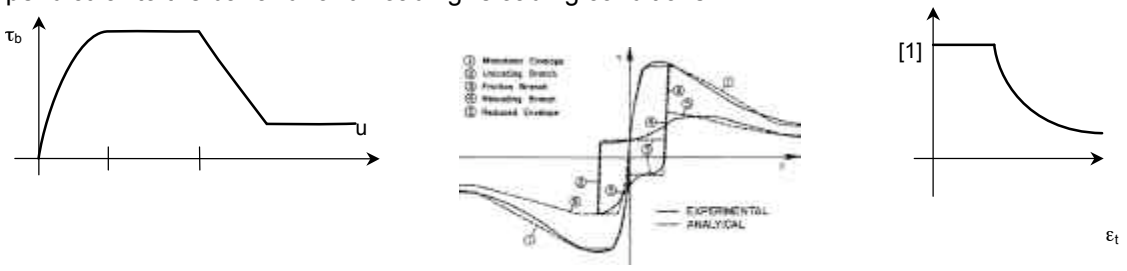

a) monotonic loading situations [13] b) for load reversals [12] c) multiplier for transversal strain [15]

Fig. 6 Bond stress - slip relation for the concrete/rebar or the tendon/grout interface

Fig. 7 shows the transmission of forces from a concrete C30/37 to a rebar ø20mm, BSt. 550. The computation was executed with the supplementary interface algorithm according to Modelcode 90 [13] for different bond conditions. The second chart in Fig. 7 presents the arising slip due the transmission of the forces. (In comparison, the basic anchorage length according to EC2 is 80cm.)

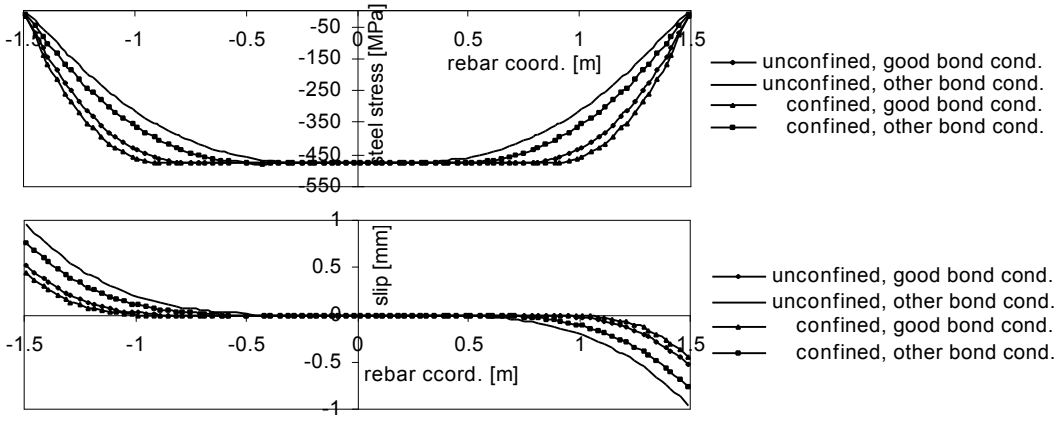

Fig. 7 Stress in the rebar versus transmission length and relative displacement (slip) according to Modelcode 90 [13] computed with the supplementary interface algorithm.

b) Interface of the tendon with the anchor

For the interface between a tendon and an anchor, a single modulus can be provided (see Fig. 8). The magnitude of this modulus should be defined to produce the wedge pull-in of the employed stressing system. This approach is favorable to setting a Diriclet boundary condition (prescribed support settlement) for the anchors, since the same theoretical framework (Eqs. (7) -(10)) can be employed. Further, wedge pull-in becomes stress dependent (similar to actual situation).

b) Interface of the tendon with the duct

For slip situations between a tendon and a duct, which can be referred to as friction is accounted for by the Mohr-Coulomb model. The wobbling effect of the tendon relates to the cohesion, see Fig. 9a. The magnitude of σ_n is obtained by relating the strains along the local configuration of the rebar ($\mathbf{e}_l$, Eq. (6)) to the constitutive relation of the concrete. Hence, $\mathbf{s}_l$ will be obtained. If the local axis of the rebar corresponds to it's moving trihedron, σ_n is the second component of $\mathbf{s}_l$. Fig. 9b shows the Mohr-Coulomb model in the bond stress – slip diagram.

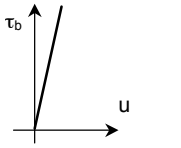

Fig. 8 Bond stress - slip relation for the anchor

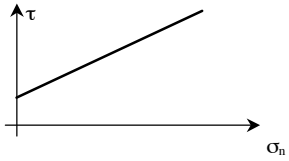

a) σ_n/τ diagram

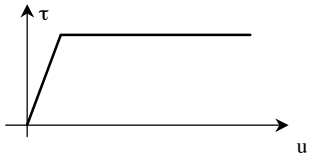

b) τ/u diagram

Fig. 9 Mohr-Coulomb Interface model

5 Application to Engineering Situations

A numerical simulation of a tensioning process can be done with the theory shown above. Numerous sequences are encountered during the whole process. On the other hand these sequences generally follow some typical procedures. For these common procedures, the program supports the user during preparation of the input data. Some cases are discussed below.

Post-Tensioned Tendons in Structural Engineering

- unbonded tendons
  Initially the Mohr-Coulomb model is established along the entire bar for the interface. Thus, a tendon can be activated at any load case, since it just slides in the duct and takes nearly no load before it is tensioned. The force of the hydraulic jack can be applied on any end or even on both ends at the same time when the tendon is jacked from both sides. When the first prestress force is applied, the interface modulus on the dead end will be set automatically to the anchorage modulus value. In all subsequent load cases on both ends, the anchorage modulus will be provided at the interfaces (a different modulus can be given as input at each end). When a second jacking action will be applied on the same tendon in any other load case, the lifting of the anchor will be modeled by setting the interface of the according end back to the Mohr-Coulomb model for this specific load case only (with the anchorage modulus reactivated thereafter).

- bonded tendons
  The procedure of applying the prestress forces is exactly the same as above. In addition, in a certain load case the ducts will be grouted and the Mohr-Coulomb model will be replaced by the interface relation given by Modelcode 90 [13]. It should be noted that this load case is the zero slip reference for the tendon/grout interface in all subsequent load cases.

- external tendons

  This kind of prestress can be accounted for by introducing a further simplification. Instead of assigning the material of the parent elements to nonlinear concrete, the external tendon can be embedded into superficial linear elastic parent elements with a negligible small modulus value.

Post-Tensioned Tendons in Geotechnical Engineering

Soil anchors have numerous applications in geotechnical engineering. Here, the simulation of soil anchors shown in Fig. 10 will be discussed. Initially, on the excavation side, the soil above the elevation of the first anchor will be excavated before any anchor can be installed. This is modeled by removing the according elements. The program applies excavation forces. In the next load case, the first anchor will be installed. On the dead end grouted conditions apply. Therefore, the prestressing force can be applied within the same load case. At the life end of the tendon, the program assumes automatically for all subsequent load cases conditions according to 4.1b. Along the portion between the life end and the dead end the Mohr-Coulomb model is employed for the tendon soil interface. The procedure for the second anchor follows accordingly.

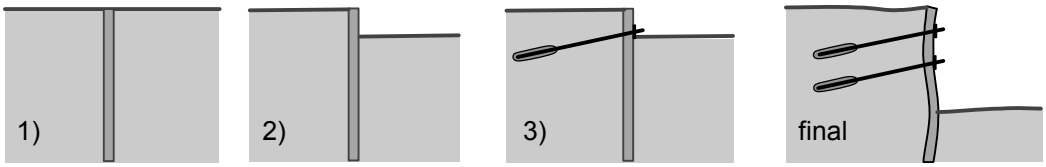

Fig. 10 Anchored retaining wall

Pre-Tensioned Tendons in Precast Concrete Members

In the construction process, prestressing forces will be induced by applying an initial tensile strain. After the concrete member has cured to a required level, the prestressing forces are transferred to the concrete. Computations start when the prestressing forces get transferred to the concrete. A grouted situation for the interface from the initial state on is employed. The tension force in the tendons will induce a compression force on the concrete. The computed slip of the wire at the end of the tendon is the wire pull-in.

6 Numerical Examples

Several case studies are currently under investigation. Although the concrete extension of the program is in an early stage of development, it is not limited to small problem sets only. Selected examples below are supposed to show the performance of the algorithm.

6.1 Effectiveness of the Supplementary Interface Algorithm

A good detailing requires the rebars to end in regions where the stress state is low. Therefore, the elements are not necessarily small in this regions. Hence, bond model should be able to account for the anchorage situation even within a big element. The calculations were carried out on one single 3D element (2m/1m/1m C30/37). The reinforcement bar (ø=20mm, BSt 550) started on the one end of the element and ended on the other end within the same element. Fig. 11 shows the capability of the implemented algorithm. It can even account for situations where the rebar starts and ends within the same element. The solid line in Fig. 11 is assumed to be a reference solution where the rebar was discretized into 20 sub elements within the parent element. For the integration six sample points along each rebar element were employed. When the rebar is modeled with only two rebar elements, the results already show the right trend. When three elements are used, the results are already within an acceptable agreement with the reference. The over estimation of the rebar stress indicated by two integration points in Fig. 11. will be cut off, if the yield stress is set to its design value. The deviation in prediction is very small when 4 rebar elements are used, as indicated in Fig. 11.

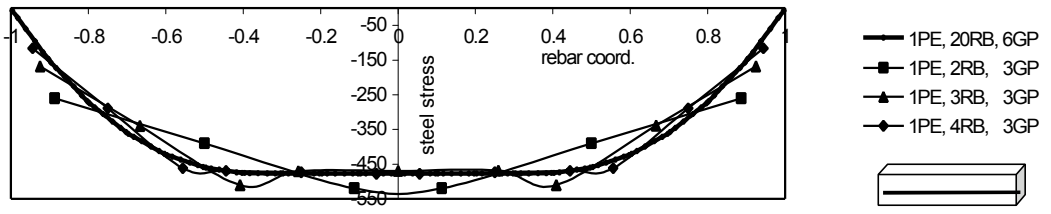

Fig. 11 Effectiveness of the Supplementary Interface Algorithm

6.2 Prestressed continuous beam with unbonded tendon

A continuous beam with an unbonded tendon subjected to a uniformly distributed vertical boundary load is shown. The concrete is modeled with Ottosen failure criterion [16] and a Rankine tension cut off.

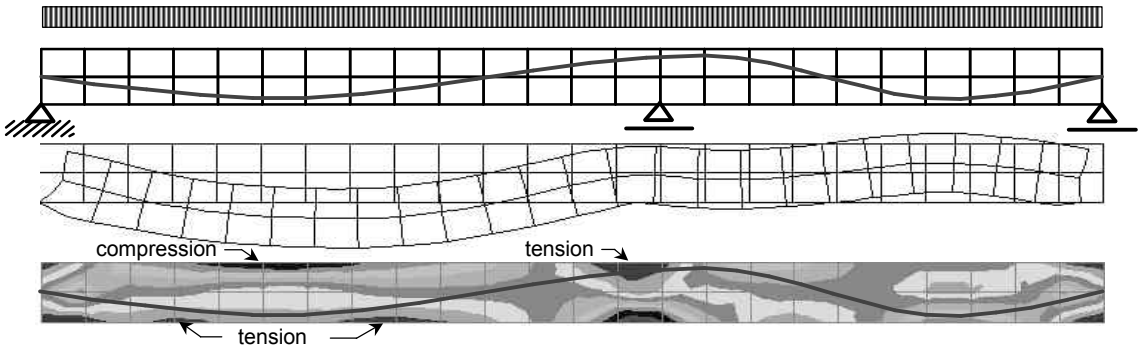

Fig. 12 Continuous beam with an unbonded tendon

6.3 Soil Structure Interaction / Tunnel Lining

The stresses in a tunnel lining are investigated here. A total of 1988 parabolic 2D elements are initially employed for the soil. The constitutive relation for the soil corresponds to Mohr-Coulomb. For 122 elements the constitutive relation is changed to concrete in load case 3 (after lowering the ground water table and excavation of the soil). The concrete is reinforced with 886 rebar elements.

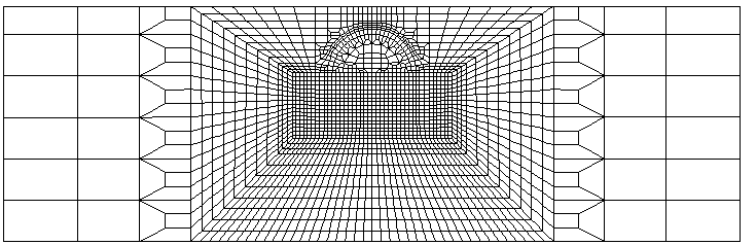

Fig. 13 Mesh with 1988 2D parabolic elements / plain strain analysis stress distribution in the concrete lining

7 Conclusion and Further Developments

Reinforced and prestressed concrete structures can be analyzed in 2D and 3D. In the two dimensional case, the program is limited to plane stress or plane strain problems. The computational effort is reasonable, but will increase somewhat when bond slip is taken into account.

Further emphasis will concentrate on modeling concrete specific phenomena such as cracking, shrinkage, creep and developing anisotropy due to load applied. On the other hand, a verification and calibration is important, and will be done by relating program results to experimental data. Finally, the capability of this model will be shown on related problems in geotechnical engineering (anchors, reinforced earth) and aspects of soil structure interaction can be investigated as well.

8 References

[1] Beer, G., “BEFE user’s and reference manual”, CSS, Graz, 1999

[2] Hartl, H, “3D Computational Modeling of Reinforced Concrete Structures with Application to Soil Structure Interaction”, Doct. Thesis, TU-Graz, in prep.

[3] Hofstetter, G., Mang, H.A., “Computational Mechanics of Reinforced Concrete Structures”, Wiesbaden, Vieweg, 1995.

[4] Elwi, A.E., Hrudey, T.M., “Finite Element Model for Curved Embedded Reinforcement”, Journal of Engineering Mechanics, ASCE, April 1989, 115(4), pp. 740-754

[5] Lin T.Y., “Load-balancing method for design and analysis of prestressed concrete structures”, Journ. ACI, V. 60, No 6, June 1963, pp. 719-742

[6] Leonhardt, F., “Vorlesungen über Massivbau”, Vol. 1-6, Springer, Berlin, 1980

[7] Ngo D., Scordelis A.C., “Finite Element Analysis of Reinforced Concrete Beams”, ACI Journal, 1967, 64, pp. 152-163.

[8] Schäfer H., “A Contribution to the Solution of Contact Problems with the Aid of Bond Elements”, Computer Methods in Applied Mechanics and Engineering, 1975, 6, pp. 335-354

[9] Hartl H., Sparowitz L, Elgamal A., “The 3D computational Modeling of Reinforced and Prestressed Concrete Structures”, 3rd International Ph.D. Symposium in Vienna, accepted, Ernst&Sohn, 2000

[10] Boresi, A. P., Schmitd, R.J., Sidebottom, O.M., “Advanced Mechanics of Materials”, Fifth Edition, Wiley, 1993

[11] Beer, G., Watson J.O., “Introduction to Finite and Boundary Element Methods for Engineers”, Wiley, 1992

[12] Eligehausen, R., Popov, E. P., Bertero, V.V., “Local Bond Stress-Slip Relationship of Deformed Bars under Generalized Excitation”, Report No. UCB/EERC-83/23, Earthquake Engineering Research Center, University of California at Berkeley, California October 1983, pp. 169

[13] CEB-FIP Comitè Euro-International du Bèton, “CEB-FIP Model Code 1990”, London, Thomas Telford, 1993

[14] Pochanart S., Harmon T., “Bond Slip Model for Generalized Excitations Including Fatigue”, ACI Material Journal, 1989, 86, pp. 465-474

[15] Priestly N., Seible F., “Seismic Assessment and Retrofit of Bridges”, UCSD Department of AMES, Report No. SSRP-9/03, July 1991

[16] Ottosen N.S., “A Failure Criterion for Concrete”, Journal of the Engineering Mechanics Division, ASCE, 1977, 103, pp. 527-535